STUDY OF A NON-INTRUSIVE ELECTRON BEAM RADIUS DIAGNOSTIC

Thomas J. T. Kwan, Barbara G. DeVolder, John C. Goldstein, and Charles M. Snell
Los Alamos National Laboratory, Los Alamos, NM 87545

Abstract

We have evaluated the usefulness and limitation of a non-intrusive beam radius diagnostic which is based on the measurement of the magnetic moment of a high-current electron beam in an axisymmetric focusing magnetic field, and relates the beam root-mean-square (RMS) radius to the change in magnetic flux through a diamagnetic loop encircling the beam. An analytic formula that gives the RMS radius of the electron beam at a given axial position and a given time is derived and compared with results from a 2-D particle-in-cell code. Our study has established criteria for its validity and optimal applications.

1. INTRODUCTION

In radiography, the x-rays are generated by an electron beam impacting a target of optimum thickness. The spot size of the electron beam before impact is an important factor in the resolution of radiography. It is therefore highly desirable to use a non-intrusive technique to measure the radius of the electron beam during its transport to obtain valuable information about the beam size on target.

2. CRITERIA OF APPLICABILITY

For the electron beam in the Integrated Test Stand (ITS) at Los Alamos National Laboratory, we have evaluated the usefulness and accuracy of the non-intrusive beam radius diagnostic proposed by W.E. Nexsen[1]. This diagnostic is based on the measurement of the magnetic moment of a high current electron beam in an axisymmetric focusing magnetic field, and relates the beam root-mean-square (RMS) radius to the change in magnetic flux through a diamagnetic loop that encircles the beam. The formula that gives the RMS radius R at a given axial position z and a given time t is[1]

$$R = \left[\frac{C|\Delta\Phi|}{B_z(0)|I_z|} \right]^{1/2} \tag{1}$$

where $\Delta\Phi \equiv \Phi(t) - \Phi(0)$, $\Phi(t)$ is the axial magnetic flux through the loop at time t, $B_z(0)$ is the external axial magnetic field at the z position of the loop, I_z is the axial particle current at z and t, and $C = 4mc\beta\gamma/\mu_o e$ is a constant in MKS units. The RMS radius R is defined by

$$R^2 I_z = \int r^2 dI_z \tag{2}$$

Using the particle-in-cell (PIC) code MERLIN, we can compare the RMS radius calculated from Eq. 1 with a code-calculated definition of R given by Eq. 2 to quantitatively evaluate the accuracy of Nexsen's diagnostic for the ITS beam. Some cautions are warranted in using this diagnostic. Nexsen's analysis is applicable to a steady-state electron beam born in a field-free region and injected into an axisymmetric magnetic field in a region with no boundaries. In applying this diagnostic to the ITS beam, we seek to use Nexsen's formula for a pinched beam with a finite risetime propagating in a drift tube. This diagnostic should be applied only after the beam current is fully risen to its peak (steady state) value and it cannot be used to measure the RMS radius of a beam immersed in a constant external magnetic field.

Equation 1 applies to unbounded systems, however, in the realistic (bounded) problem, the magnetic flux diffusion time is nonzero across boundary materials. On the time scales set by the ITS beam, flux displaced from the initial configuration (external magnetic field only), due to the presence of the propagating beam, cannot penetrate the drift tube wall. That is, for a beam propagating inside a drift tube and in an external solenoidal field, the total flux within the drift tube is conserved. For a diamagnetic beam, the total magnetic field inside the beam decreases below the value of the external field, and this is compensated by an increase in the field in the vacuum region between the beam and the drift tube wall. The complex dynamics of the beam propagating in the external and self fields may also produce regions in space where the field inside the beam exceeds the external field there, so that the beam is non-diamagnetic. In either case, the total flux is conserved within the drift tube. The presence of the flux-conserving wall modifies the flux change $\Delta\Phi$ in Eq. 1, which is applicable to an unbounded system. To use Nexsen's diagnostic in the case of a beam propagating inside a drift tube, we must adjust the code-calculated flux change for a bounded system in order to use Eq. 1. By inserting a flux-adjustment-factor (FAF) that depends on the loop and drift tube radii, we increase the magnetic flux $|\Delta\Phi|$ change to correspond to that which is appropriate to an unbounded system. This factor can be approximately derived [2] to be

$$FAF = \left[1 - \frac{A(loop}{A(drift)} \right]^{-1/2} \tag{3}$$

where A(loop) is the area of the diamagnetic loop and A(drift) is the area of the drift tube. This geometric flux-

0-7803-4376-X/98/$10.00

adjustment-factor (Eq. 3) must be applied to Eq. 1 in order to use the diagnostic for a beam propagating in a drift tube. The flux change $\Delta\Phi$ in Eq. 1 varies with the axial location of the loop in the external magnetic field. When the loop is located in a region of small external field (say, near the ends of the solenoidal coils), the value of $\Delta\Phi$ is a small number (being the difference of two nearly equal numbers). The code-calculated flux is noisy, and the noise reduction procedure used to calculate a value for $\Phi(t)$ is somewhat arbitrary and may therefore produce non-unique values for $\Delta\Phi$. Such values of $\Delta\Phi$ could therefore be uncertain by 25% or more, and this fact will introduce uncertainties in the RMS radius calculated from Eq. 1. Locating the diamagnetic loop in a region of peak external magnetic field ensures larger flux and flux change $\Delta\Phi$, often larger by an order of magnitude or more. These larger values reduce the uncertainty in the calculated RMS radius. Therefore, the diamagnetic loop should be placed in a region of maximum external magnetic field. The flux change $\Delta\Phi$ in Eq. 1 also varies with loop radius, being largest when the loop radius approaches the beam radius. Because of the arbitrariness and uncertainty introduced in calculating $\Delta\Phi$ as the small difference of two nearly equal numbers, better accuracy for R is ensured for larger values of $\Delta\Phi$. In the limit that the loop radius approaches the drift tube radius, the flux change is zero because the total flux enclosed by such a loop is conserved. Furthermore, the FAF is a maximum (namely, infinity) as A(loop) approaches A(drift), but is a minimum as A(loop) approaches its minimum allowed value of A(beam), where A(beam) is the cross-sectional area of the beam at the axial location of the loop. The nature of the FAF is that of a back-of-the-envelope calculation, in that time and space variations of the fields and the particle positions are not taken into account. Hence, situations where the FAF is a minimum (i.e., the adjustment necessary to apply code-calculated quantities to Nexsen's formula for an unbounded system is a minimum) are more appropriate. For a given diamagnetic loop, the difference between the loop radius and the beam radius is largest at the pinch, and the corresponding $\Delta\Phi$ will be small and highly uncertain. In addition, the strongly two-dimensional behavior of the pinched electron beam casts doubt on the validity of Eq. 1 in this region. Therefore, the diamagnetic loop radius should be close to (but greater than) the beam radius. The diagnostic is not suited for measuring the RMS radius at or near the pinch.

The simulations described in the following section help to quantify the term "close" for the ITS beam. Accuracy to within a few percent can be achieved when the loop radius is within a couple of centimeters of (and larger than) the beam radius. When the loop radius is more than a couple of centimeters larger than the beam radius, such as when the loop is located close to the drift tube wall, then errors may be greater than 10%.

In summary, Nexsen's analysis is based on a steady state, unbounded system, and the formula in Eq. 1 must be applied to a bounded, flux-conserving experiment (and simulation). To accomplish this with reasonable confidence in the diagnostic, the loop should be placed far from the pinch, in a region of maximum external magnetic field, and should use a diamagnetic loop that is within a couple of centimeters of the beam radius (and encircles the entire beam). Because the location of the pinch is a priori unknown and depends on the initial beam radius and on the initial angle of the beam envelope, the simulations can play a crucial role in evaluating the accuracy of the diagnostic data. Moreover, since the experimentalist is limited to locating the diagnostic loop close to the drift tube wall, in order to ensure that the loop surrounds the entire beam, the code can serve as an essential benchmarking tool to correlate the RMS radius determined from the (experimental) large-radius loop with that determined from simulation loops whose radii are closer to the beam radius.

3. MERLIN SIMULATIONS

The ITS beam was modeled using the 2-1/2-dimensional PIC code MERLIN. The typical geometry used in the simulations, assumed axisymmetric, is depicted in the Fig. 1.

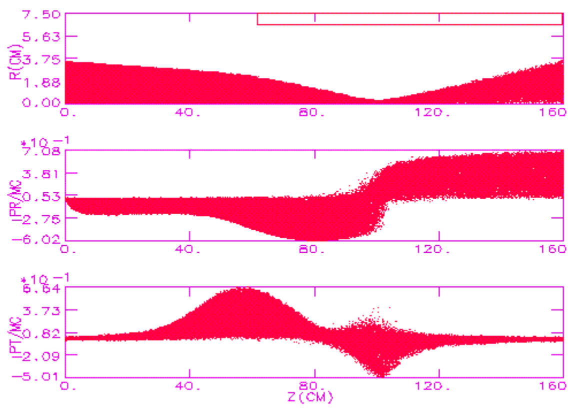

Figure 1. Configuration and phase space plots of a typical simulation at 16.7ns.

The drift tube radius is 7.5 cm, and the axial extent is 160 cm. A solenoid of length 13.125 inches is energized to produce a peak axial magnetic field of approximately 1 kG. This field was generated with the code BFIELD, which links to MERLIN, by specifying 35 current loops approximately uniformly distributed between z = 45.33 cm and z = 78.67 cm. positions. The magnetic field varies slightly with r in the vicinity of the maximum field, which is the location of diagnostic probes in both simulation and experiment. This small variation violates the assumption in the previous analysis and may introduce slight errors.

The electron beam has uniform initial density for $r \leq r_b$, the beam radius. The peak current is about 3 kA, with a 3-ns risetime and a flat top: the functional dependence used in MERLIN is $I(t) = I_o [1-\exp(-0.5(t/\tau)^2]$ where τ is the 3-ns risetime. The electrons' initial kinetic energy is 5.31 Mev, which corresponds to a γ of 11.39. In ITS, a metal annular sleeve of thickness about 1 cm fits tightly into the drift tube and holds the diamagnetic loop, which is embedded in plastic. This sleeve is simulated as a 1-cm-thick conductor that extends from the position of maximum external magnetic field (z = 61.8 cm) to the downstream boundary at z = 160 cm as shown in Fig. 1. The numerical probes in the simulations to calculate the RMS radius are located at the z-position of maximum external field and at two different radial positions, 4.0 and 6.0 cm. Two radial locations were chosen, because the larger radius corresponds to the experiment and because the smaller-radius loop will allow us to quantify the improved accuracy of the calculated RMS radius resulting from the loop radius being closer to the beam radius.

We set up our simulations according to experimental observation that the range of initial beam radius is 2.5 - 4.0 cm, and the range of initial angle of the beam envelope (dr/dz) is ± 60 milliradians. In addition, we imposed an arbitrary initial Gaussian scatter of 1 milliradian on the beam for all cases.

Application of Eq. 1 requires the difference in magnetic flux at two times, t = 0 and some t > 0 at which the RMS radius of the beam is being calculated. Even in the region of maximum external magnetic field, the flux difference is a small number, typically for ITS parameters only a fraction of a percent of the absolute value of the flux. Although the flux at t = 0 can be determined exactly from the simulations, the flux at t > 0 is more uncertain and must be carefully processed to minimize numerical flux noise resulting from the simulations. Figure 2 is an example of the magnetic flux in one of the simulations.

Table 1 summarizes the results of nine simulations with various initial beam radii and angles of the injected beam envelope. It compares the RMS radius using Eq. (1) and the definition Eq. (2) for the nine simulations. The probes were placed at the axial position corresponding to maximum external magnetic field (z = 61.8 cm) and radial positions r = 4.0 cm (smaller diamagnetic loop to demonstrate increased accuracy) and r = 6.0 cm (larger diamagnetic loop typically used in experiments). The RMS radius is calculated at 16.2 ns, which is in the steady-state regime.

Except in cases where the particles' large radial positions render the diagnostic meaningless (a and b), we calculate three values of the RMS radius for each simulation: the definition and the Nexsen values at r = 4.0 and 6.0 cm. Error bars for the Nexsen RMS radii in Table 1 are certainly nonzero, but cannot be accurately quantified because the errors associated with the calculation of the flux change can only be roughly estimated. Better agreement is obtained when the loop radius is closer to the beam radius.

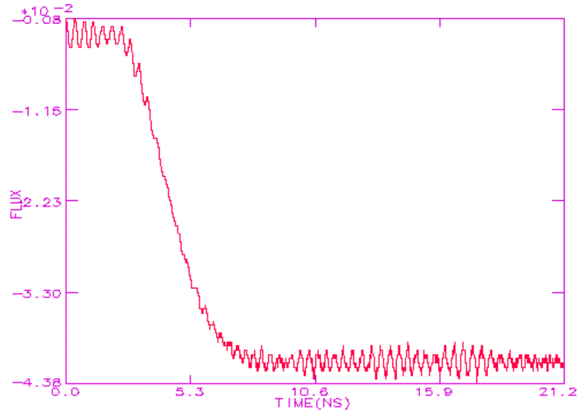

Figure 2. Example of magnetic flux, as a function of time, through a 4.0-cm loop located at the axial position of peak external magnetic field.

Table 1

r_0(cm)/θ_0(mrad)	RMS Radius (cm)		
	Definition	4.0 cm loop	6.0 cm loop
3.5	1.46	1.46	1.46
3.5/-60	1.18	1.21	1.35
3.5/63	4.00	a	3.12
4.0/0	1.80	1.79	1.68
2.5/0	0.79	0.90	1.19
4.0/-69	1.21	1.22	1.34
2.5/-42	1.11	1.18	1.30
4.0/71	4.66	b	b
2.5/45	2.58	2.52	2.16

4. CONCLUSIONS

In our study, we find that the accuracy of the RMS radius probe increases when the diamagnetic loop is far from the metal wall (close to the beam radius). A convenient rule-of-thumb, based on this limited set of data, is that placing the diamagnetic loop within a couple of centimeters of the beam radius is sufficient to ensure reasonable accuracy.

5. ACKNOWLEDGMENTS

We wish to acknowledge Dave Moir and Evan Rose for many useful discussions throughout this work.

6. REFERENCES

[1] W. W. Nexen, "A Non-Interfering Beam Radius Diagnostic," draft paper dated August 19, 1991.

[2] W. E. Nexsen, "Beam Brightness from Beam Diamagnetism," unpublished LLNL research memo 87-27, August 7, 1987.